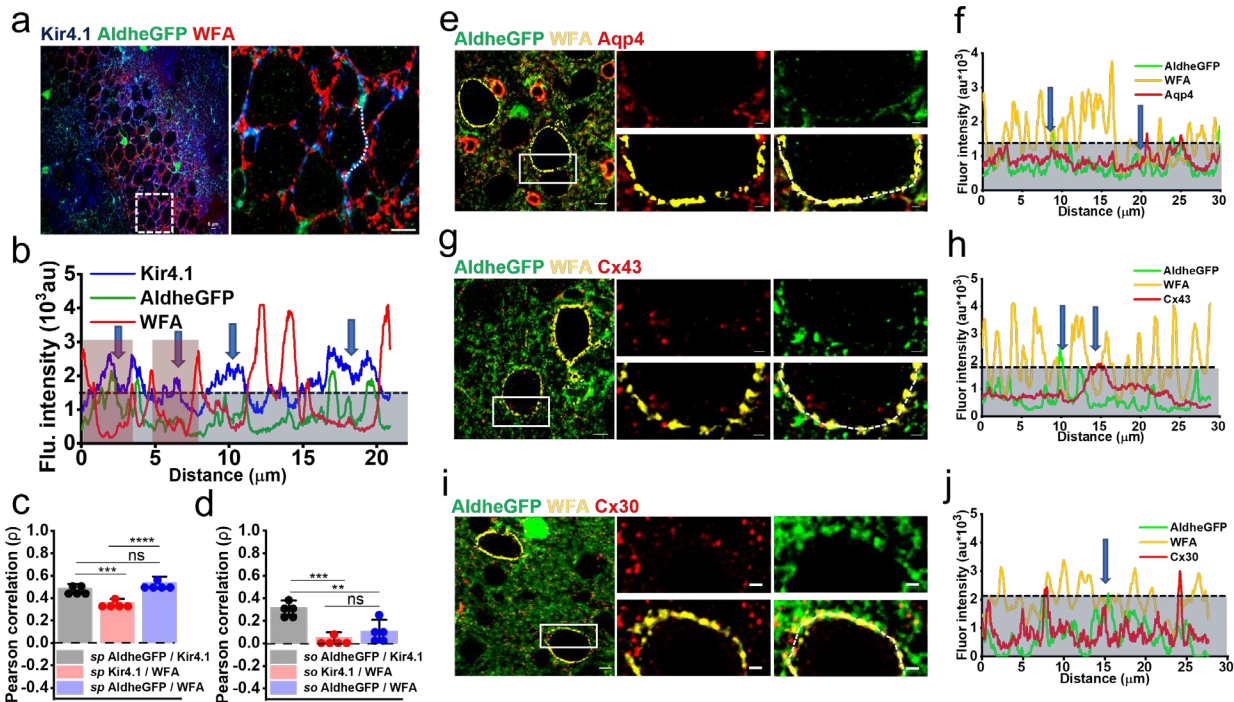


1214 **Supplementary figures**

1215



1216
1217

Fig. S1 In CA2 of hippocampus, PNNs holes contain astrocytic processes.

1218 **a** Representative confocal micrographs showing hippocampal CA2 PNNs (WFA - red)
1219 and astrocytes labelled with AldheGFP (green) and Kir4.1 (blue). The right image shows
1220 the magnified area of the white square in left large image. Scale bar 5μm.

1221 **b** Line intensity profiles of the white dotted line drawn in Fig. **a** (right), showing
1222 fluorescence intensity of PNN and astrocytic markers. Blue arrows point to the PNN holes
1223 occupied by astrocytic processes expressing Kir4.1. Red bars in between two
1224 consecutive WFA peaks represent the area of PNN holes wherein astrocytic processes
1225 can be confined.

1226 **c-d** Bar diagrams showing Pearson correlation of spatial overlap between astrocytic
1227 markers AldheGFP and Kir4.1 with each other and with PNN marker WFA in **c** stratum
1228 pyramidale (Kir4.1-AldheGFP 0.49 ± 0.03 , Kir4.1-WFA 0.36 ± 0.02 , AldheGFP-WFA 0.53
1229 ± 0.05) and **d** stratum radiatum of CA2 (Kir4.1-AldheGFP 0.31 ± 0.06 , Kir4.1-WFA $0.05 \pm$
1230 0.04 , AldheGFP-WFA 0.10 ± 0.10). $n = 5$ sections/5 mice, **** $P < 0.0001$, *** $P < 0.001$,
1231 ** $P < 0.01$, * $P < 0.05$, ns = $P > 0.05$. One-way ANOVA, Tukey's post-hoc test. Bar data
1232 are expressed as mean \pm SD; dots on the bars represent the individual data points.

1233 **e** Representative confocal micrographs showing expression of aquaporin 4 (red) in
1234 astrocytic processes (AldheGFP – green) in holes of cortical PNNs (WFA - yellow). The
1235 right side panels show the magnified area marked by a white rectangle in the left image.

1236 **f** Intensity profiles of the white dotted line drawn on the PNN (bottom right panel)
1237 represented PNN holes (marked by blue arrows) occupied with astrocytic processes
1238 (AldheGFP-green) expressing Aqp4 (red).

1239 **g** Representative confocal micrographs showing expression of connexin 43 (red) in
1240 astrocytic processes (AldheGFP – green) in holes of cortical PNNs (WFA - yellow). The
1241 right side panels show the magnified area marked by the white rectangle in the left image.

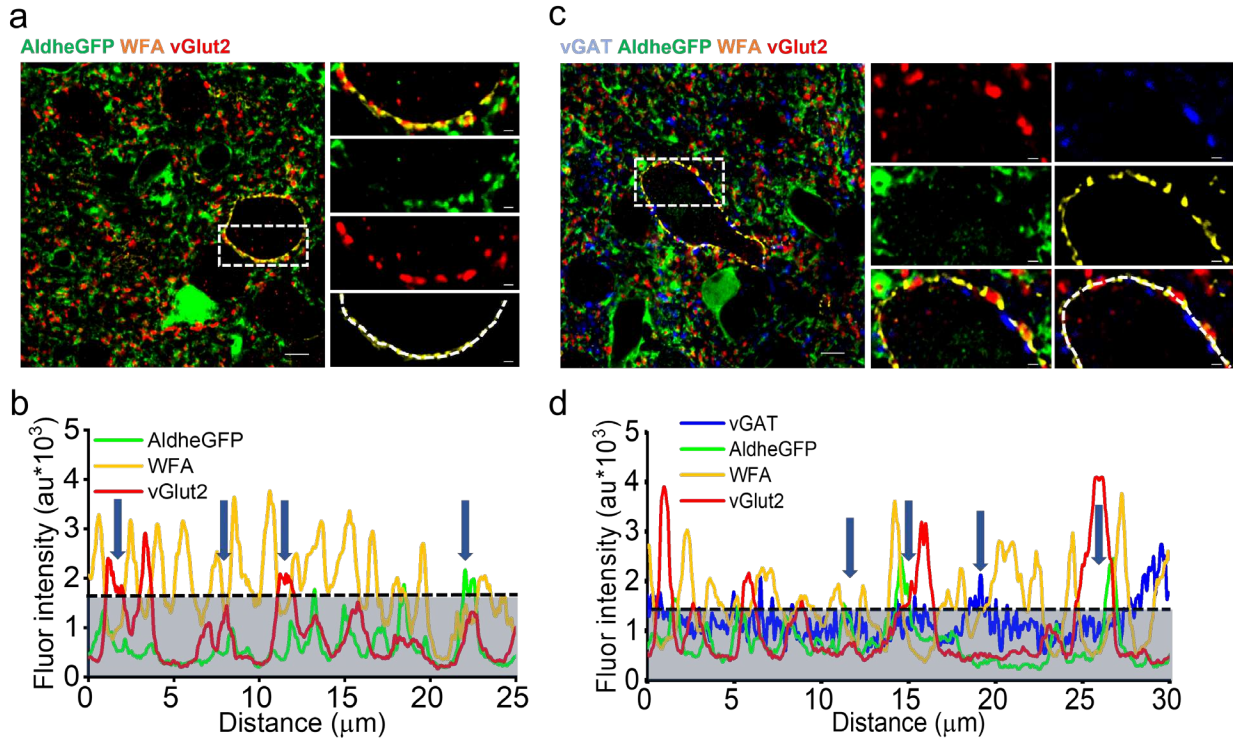
1242 **h** Intensity profiles of the white dotted line drawn on the PNN (bottom right panel)
1243 represented PNN holes (marked by blue arrows) occupied with astrocytic processes
1244 (AldheGFP-green) expressing connexin 43 (red).

1245 **i** Representative confocal micrographs showing expression of connexin 30 (red) in
1246 astrocytic processes (AldheGFP – green) in holes of cortical PNNs (WFA - yellow). The
1247 right side panels show a magnified area marked by the white rectangle in left image.

1248 **j** Intensity profiles of the white dotted line drawn on the PNN (bottom right panel)
1249 represented PNN holes (marked by blue arrows) occupied with astrocytic processes
1250 (AldheGFP-green) expressing connexin 30 (red).

1251 Scale bars 5 μ m in large images, 1 μ m in magnified images in e-i. Blue area under the
1252 dotted lines in line profiles in b, f, h, and j represents the WFA threshold.

1253



1254
1255
1256

Fig. S2 PNN holes contain astrocytic processes and thalamocortical synaptic contacts.

1257 **a** Representative confocal micrographs showing expression of vGlut2 (red) expressing
1258 synapses as well as astrocytic processes (AldheGFP – green) in holes of cortical PNNs
1259 (WFA - yellow). Right side panels show a magnified area marked by the white rectangle
1260 in left image.

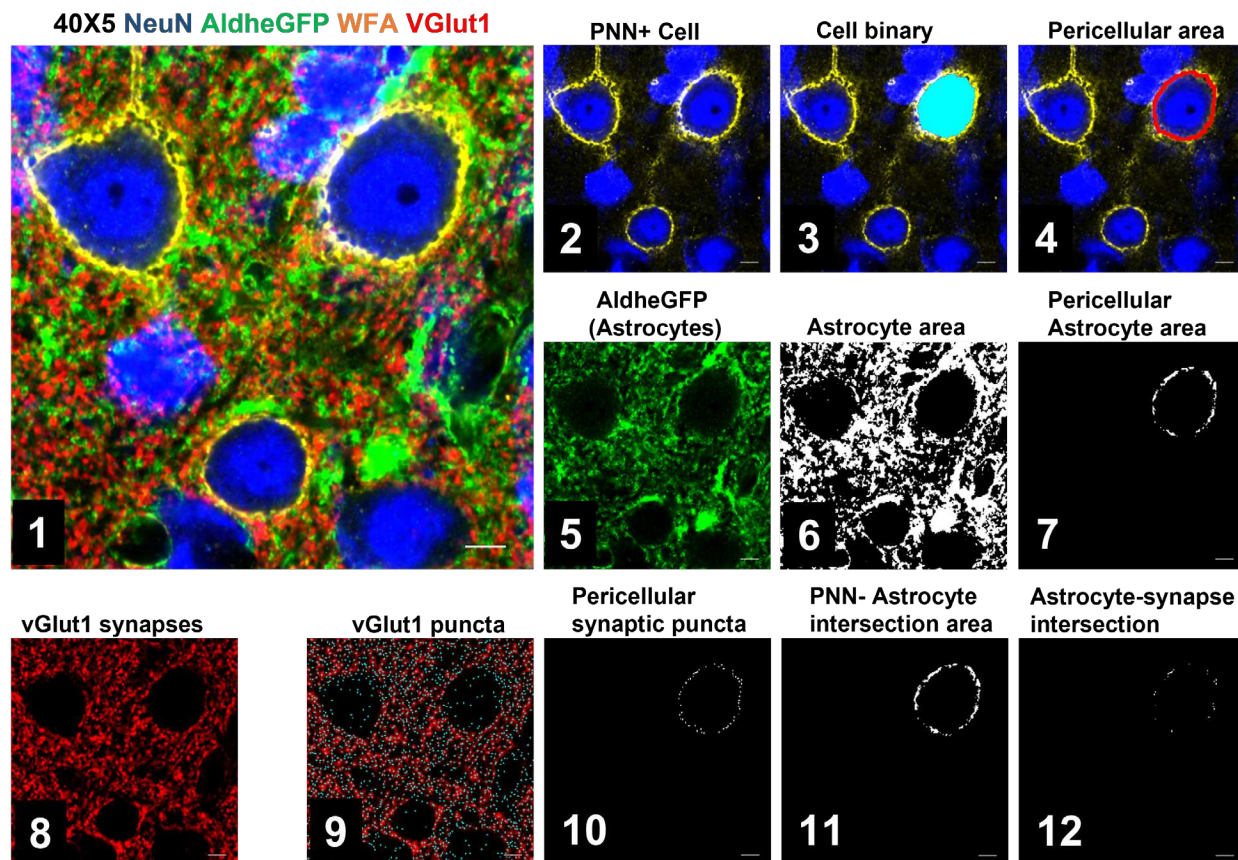
1261 **b** Intensity profiles of the white dotted line drawn on the PNN (bottom right panel)
1262 represented PNN holes (marked by blue arrows) occupied with astrocytic processes
1263 (AldheGFP-green) and vGlut2 expressing synapses (red).

1264 **c** Representative confocal micrographs showing expression of glutamatergic (vGlut2 -
1265 red) and GABAergic (vGAT - blue) synapses as well as astrocytic processes (AldheGFP
1266 – green) in holes of cortical PNNs (WFA - yellow). Right side panels show a magnified
1267 area marked by the white rectangle in left image.

1268 **d** Intensity profiles of the white dotted line drawn on the PNN (bottom right panel)
1269 represented PNN holes (marked by blue arrows) occupied with astrocytic processes
1270 (AldheGFP-green) and glutamatergic (vGlut2 - red) and GABAergic (vGAT - blue)
1271 synapses.

1272 Scale bar 5μm in large images, 1μm in magnified images in both a and c. Blue area under
1273 the dotted lines in line profiles in b and d represents the WFA threshold.

1274



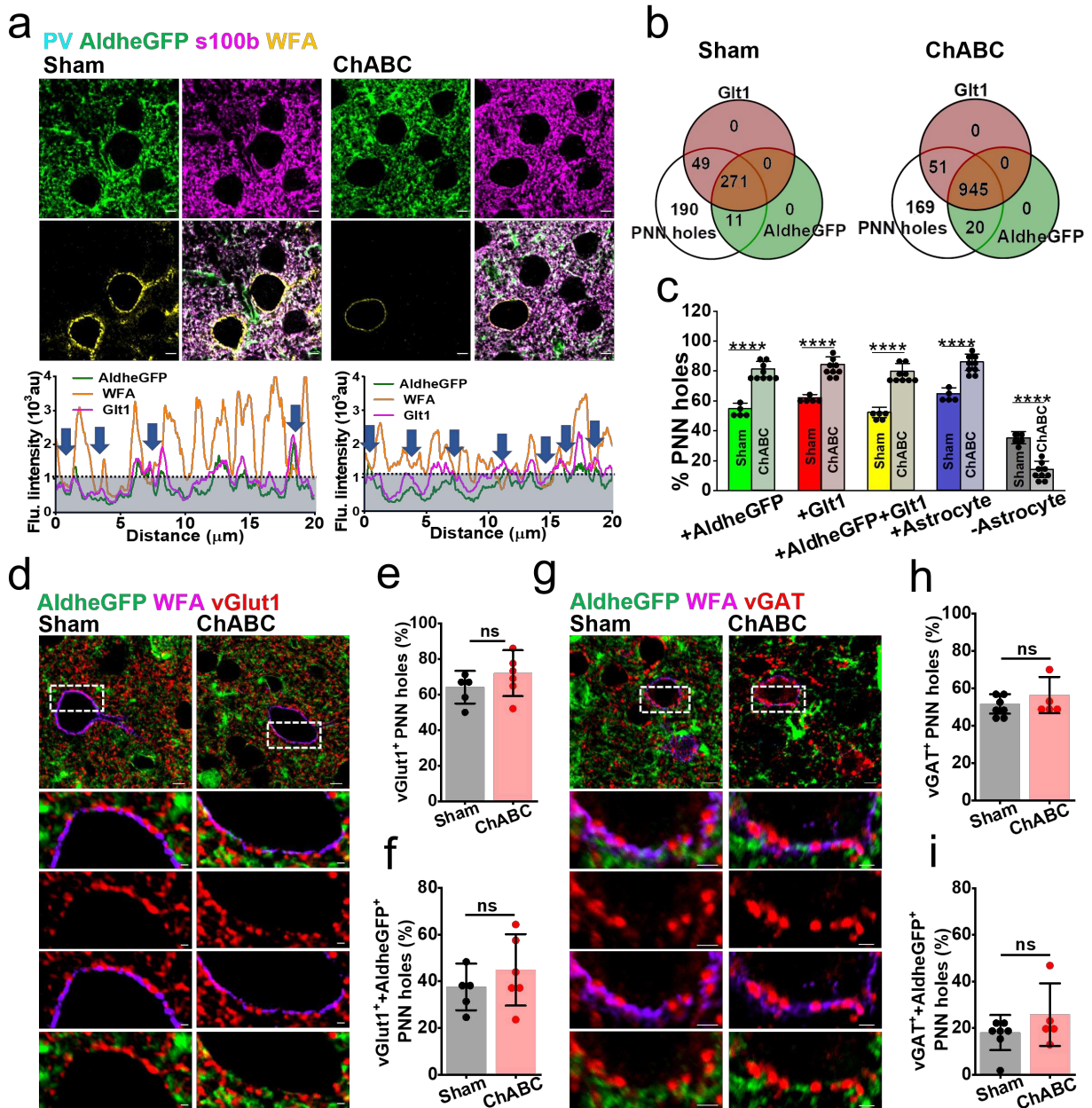
1275
1276

Fig. S3 Pericellular astrocytic coverage and synaptic contacts analysis method.

1277 Multichannel confocal image (1), showing immunofluorescence labeling of neurons
1278 (NeuN), astrocytes (AldheGFP), PNNs (WFA), and synaptic terminals (vGlut1). The NeuN
1279 signal of the soma of PNN-expressing neurons (2), is binarized (3), and the pericellular
1280 0.8 - 1µm area (4) is defined. AldheGFP signal (5), is binarized using automated OTSU
1281 function (6), and pericellular AldheGFP area (7), is extracted by intersecting (4) and (6)
1282 binary images. Synaptic marker vGlut1 (8), image is processed with an automated peak
1283 detection function to detect vGlut1 puncta (8). Intersecting (9) with (4) generates
1284 pericellular synaptic puncta (10). Intersecting the PNN signal with (7) generates a PNN-
1285 astrocyte intersection area (11), and intersecting (7) with (10) generates vGlut1 puncta in
1286 contact with the pericellular astrocytic area (12). Scale bar: 5µm.

1287

1288



1289
1290
1291

Fig. S4 Astrocytic processes occupy newly formed PNN holes after ChABC treatment.

1292 **a** Confocal micrographs showing immunofluorescence of astrocytes (AldheGFP – green),
1293 astrocytic glutamate transporter Glt1 (magenta), and PNNs (WFA - yellow), from sham
1294 and ChABC-injected mouse cerebral cortex. Scale bar 5 μ m. Line intensity profiles of a
1295 typical PNN from sham (left) and ChABC treated (right) conditions showing low WFA
1296 intensity and high occupancy of PNN perforations with astrocytic processes. Blue area
1297 under the dotted line represents the threshold WFA intensity.

1298 **b** Venn diagrams showing the proportional occupancy of PNN holes by astrocytic
1299 processes (AldheGFP + Glt1) in sham (left) and ChABC-treated (right) conditions.

1300 **c** Bar diagram showing the percent of total PNN holes in sham and ChABC treated groups
1301 occupied by AldheGFP (Control 54.76 ± 3.75 , ChABC 81.05 ± 5.24), Glt1 (Control 62.09
1302 ± 2.16 , ChABC 84.15 ± 5.26) and both (Control 52.32 ± 3.50 , ChABC 79.64 ± 5.38), any
1303 astrocytic marker positive (Control 64.67 ± 4.09 , ChABC 85.80 ± 5.51) and any astrocytic
1304 marker negative (Control 35.32 ± 4.09 , ChABC 14.19 ± 5.51) holes. $n \geq 40$ PNNs/8s/4m
1305 in each group.

1306 **d** Confocal micrographs showing immunofluorescence of astrocytes (AldheGFP – green),
1307 excitatory terminals vGlut1 (red), and PNNs (WFA - magenta), from sham and ChABC-
1308 injected mouse brains. Magnified images of different combinations showing synaptic
1309 contacts in PNN holes in sham and ChABC-injected mouse brains. Scale bar $5\mu\text{m}$ in the
1310 large image, $1\mu\text{m}$ in magnified images.

1311 **e** Pericellular density of vGlut1 terminal in the PNN holes in the ChABC-treated group
1312 remained unaltered compared to sham (Control 64.10 ± 9.14 , $n = 22$ PNNs/5m, ChABC
1313 71.98 ± 12.89 , 35PNNs/5m).

1314 **f** Pericellular density of vGlut1 terminal with astrocytic contacts in the PNN holes in
1315 ChABC treated group remained unaltered compared to sham (Control 37.58 ± 9.97 , $n =$
1316 22 PNNs/5m ChABC 44.87 ± 15.29 , 35PNNs/5m).

1317 **g** Confocal micrographs showing immunofluorescence of astrocytes (AldheGFP – green),
1318 inhibitory terminals vGAT (red), and PNNs (WFA – magenta), from sham and ChABC-
1319 injected mouse brains. Magnified images of different combinations showing synaptic
1320 contacts in PNN holes in sham and ChABC-injected mouse brains. Scale bar $5\mu\text{m}$ in the
1321 large image, $1\mu\text{m}$ in magnified images.

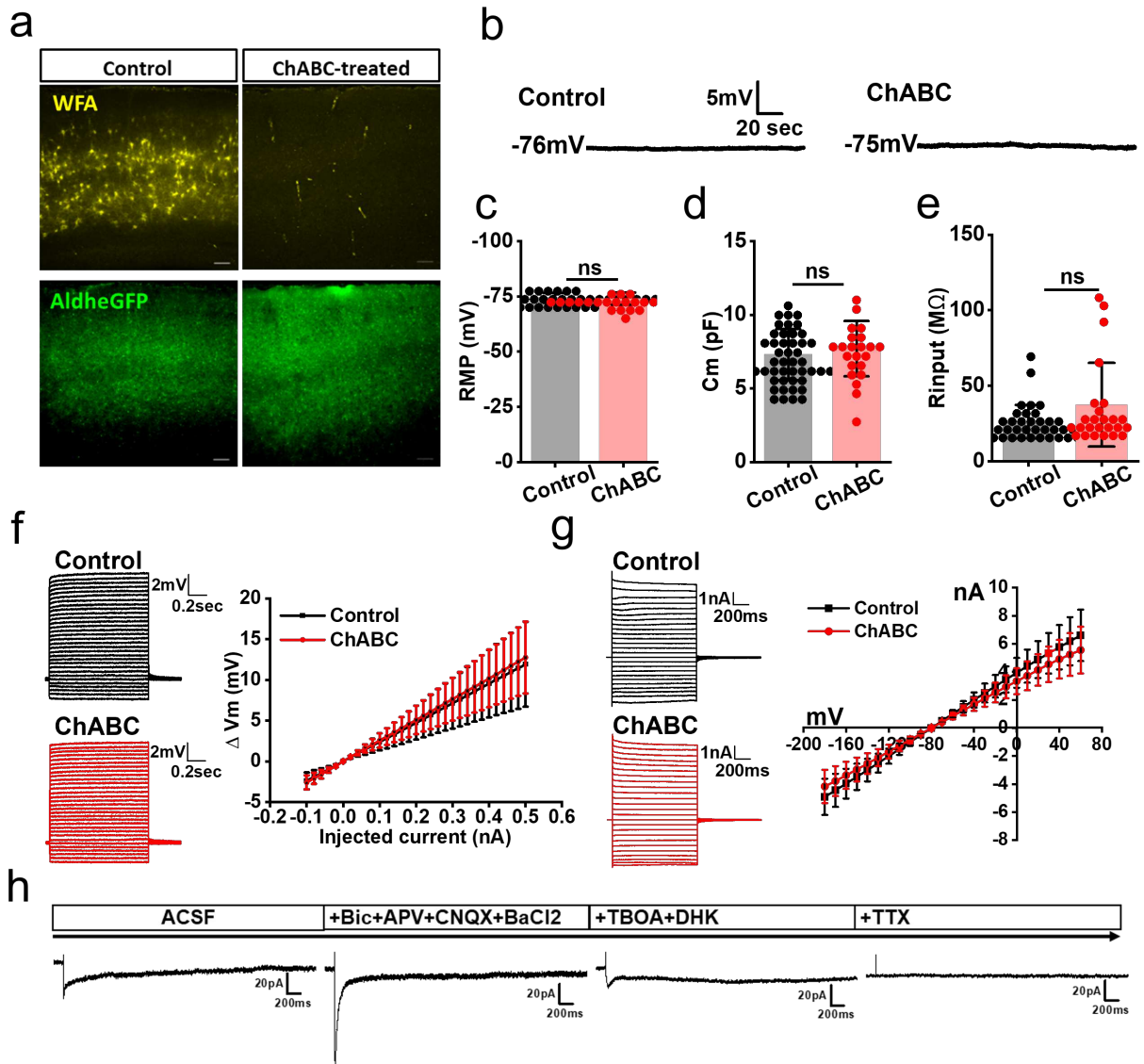
1322 **h** Pericellular density of vGAT terminal in the PNN holes in ChABC treated group
1323 remained unaltered compared to sham (Control 51.62 ± 5.20 , $n = 40$ PNNs/6m; ChABC
1324 56.36 ± 9.69 , 26PNNs/5m).

1325 **i** Pericellular density of vGAT terminal with astrocytic contacts in the PNN holes in ChABC
1326 treated group remained unaltered compared to sham (Control 18.11 ± 7.53 , $n =$
1327 22 PNNs/5m ChABC 25.81 ± 13.43 , 35PNNs/5m).

1328 s and m indicate the number of sections and mice respectively. ****P < 0.0001, ***P <
1329 0.001, **P < 0.01, *P < 0.05, ns = P > 0.05. One-way ANOVA, Tukey's post-hoc test in d;
1330 Unpaired two-tailed t-test with Welch's correction in f, g, i, and j. Bar data are expressed
1331 as mean \pm SD; dots represent individual data points.

1332

1333



1334
1335
1336

Figure S5. Biophysical properties of astrocytes remain unchanged on PNN disruption with ChABC.

1337 **a** Confocal images of WFA and AldheGFP fluorescence in control and ChABC-treated
1338 acute slices fixed and stained after electrophysiological recordings. Scale 100μm.

1339 **b** Representative current-clamp traces of astrocytic resting membrane potential from
1340 control and ChABC-treated slices.

1341 **c - e** Bar diagrams showing unchanged (**c**) resting membrane potential (control $-74.47 \pm$
1342 2.24mV , $n = 49\text{c}/18\text{m}$; ChABC $-74.04 \pm 2.7\text{mV}$, $24\text{c}/6\text{m}$), (**d**) membrane capacitance
1343 (control $7.29 \pm 1.3\text{pF}$, $n = 46\text{c}/17\text{m}$, ChABC 7.70 ± 1.8 , $n = 22\text{c}/7\text{m}$), and (**e**) input
1344 resistance (control $-26.29 \pm 37.46\text{m}\Omega$, $n = 41\text{c}/18\text{m}$; ChABC $-37.46 \pm 27.69 \text{m}\Omega$, $25\text{c}/7\text{m}$)
1345 of astrocytes in ChABC treated slices compared to control slices. ns signifies $P > 0.05$,
1346 Unpaired two-tailed student's t-test with Welch correction in **c - e**.

1347 **f** Representative current clamp traces and IV plot showing the current-voltage relationship
1348 of astrocytes in control (n = 49c/18m) and ChABC treated (n = 28c/9m) slices.

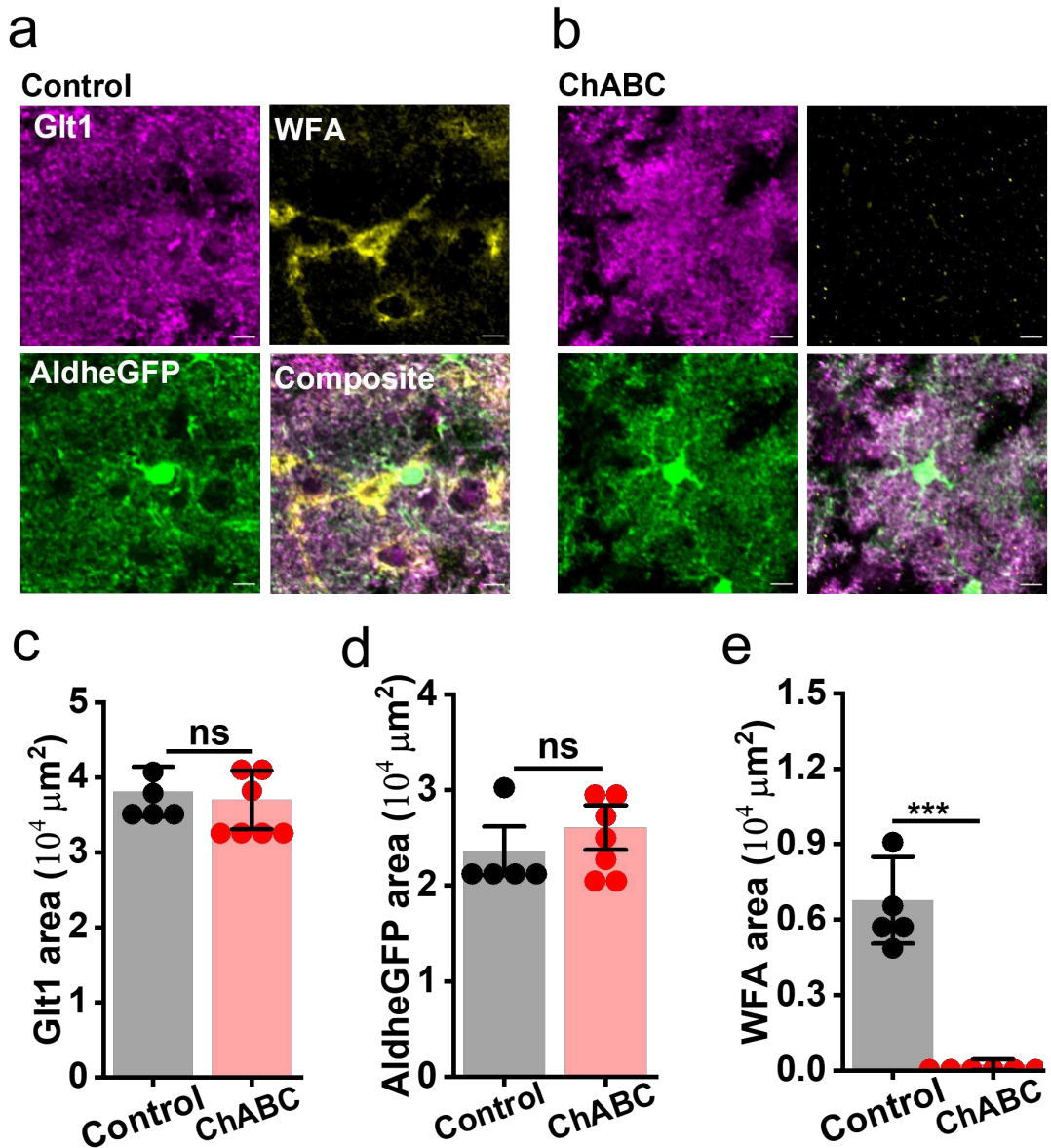
1349 **g** Representative voltage clamp traces, and IV plot showing the current-voltage
1350 relationship of astrocytes in control (n = 59c/18m) and ChABC treated (n = 38c/8m) slices.

1351 **h** Representative voltage clamp traces of synaptically evoked currents in astrocytes in
1352 presence of different blockers to isolate glutamate current.

1353 c and m represent the number of cells and mice respectively.

1354

1355



1356

1357 **Figure S6. Unaltered glutamate transporter expression on PNN depletion in acute**
 1358 **brain slices.**

1359 **a - b** Confocal micrographs of Glt1 (magenta), aldheGFP (green), and WFA (yellow)
 1360 fluorescence from fixed acute slices from control (**a**) and after ChABC treatment (**b**). Scale
 1361 bar 10 μm .

1362 **c-e** Bar diagrams of immunofluorescence area of, (**c**) Glt1 (control 38077.65 ± 3342.90 ;
 1363 ChABC 36986.21 ± 3914.77), (**d**) AldheGFP (control 23635.67 ± 3772.71 , ChABC
 1364 26070.47 ± 4100.87), and (**e**) WFA (control 6769.05 ± 1723.79 , ChABC 226.70 ± 214.73)
 1365 showing PNN disruption without any changes in astrocytic Glt1 expression. Control n =
 1366 5s/3m; ChABC 7s/3m in c-e. Units, μm^2 in c-e.

1367 s and m represent the number of slices and mice respectively. ****P < 0.0001, ***P <
1368 0.001, **P < 0.01, *P < 0.05, ns = P > 0.05. unpaired two-tailed student t-test (equal
1369 variance not assumed). Bar data are expressed as mean±SD; dots on the bars represent
1370 the individual data points.